TSSA in heavy flavour production as a probe of Gluon Sivers Function.

Rohini M. Godbole
Centre for High Energy Physics, IISc, Bangalore, India

1. Transverse Single Spin Asymmetry : TSSA.

2. TMD's : GPM, why the Gluon Sivers Function?

3. Connection: Heavy flavour and Gluons

4. $ep^{\uparrow}$ and $pp^{\uparrow}$ processes.

5. Some results. More details of some of the results present in talk by Abhiram Kaushik and Posters by Bipin Sonawane et al.

Based on:

1)R. M. Godbole, A. Misra, A. Mukherjee and V. S. Rawoot, "Sivers Effect and Transverse Single Spin Asymmetry in $e+p^{\uparrow} \to e+J/\psi+X$," Phys. Rev. D **85** (2012) 094013

2)R. M. Godbole, A. Misra, A. Mukherjee and V. S. Rawoot, "Transverse Single Spin Asymmetry in $e+p^{\uparrow} \to e+J/\psi+X$ and Transverse Momentum Dependent Evolution of the Sivers Function," Phys. Rev. D **88** (2013) no.1, 014029

3)R. M. Godbole, A. Kaushik, A. Misra and V. S. Rawoot, "Transverse single spin asymmetry in $e+p^{\uparrow} \to e+J/\psi+X$ and Q^2 evolution of Sivers function-II," Phys. Rev. D **91** (2015) no.1, 014005.

4)R. M. Godbole, A. Kaushik and A. Misra, "Transverse single spin asymmetry in $p + p^{\uparrow} \to D + X$," Phys. Rev. D **94** (2016) no.11, 114022

5) R. M. Godbole, A. Kaushik, A. Misra, V. Rawoot and B. Sonawane, "Transverse Single Spin Asymmetry in $p+p^{\uparrow} \to J/\psi+X$," arXiv:1703.01991 [hep-ph].

6)R. M. Godbole, A. Kaushik and A. Misra, "Transverse single-spin asymmetry in the low-virtuality leptoproduction of open charm as a probe of the gluon Sivers function," arXiv:1709.03074 [hep-ph].

TSSA arise in scattering of unpolarised probes (electron or proton) off transversely polarised proton.

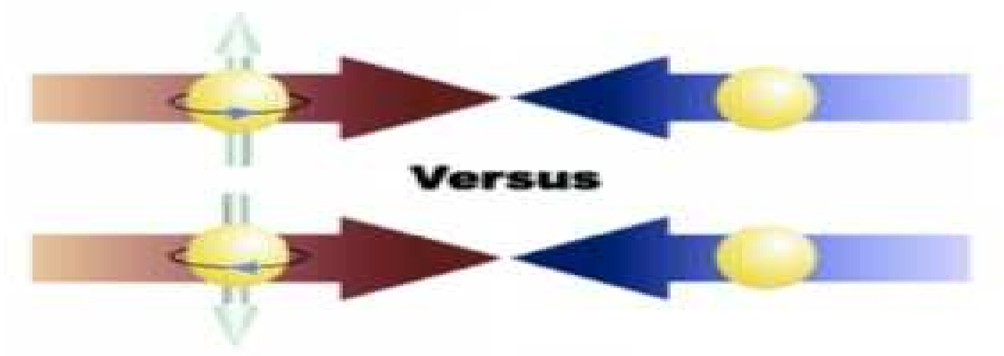

Final observed hadrons have asymmetric distribution in the transverse plan perpendicular to the beam direction depending on the polarisation vector of the scattering nucleon.

Consider Inclusive scattering: $A^{\uparrow} + B \rightarrow C + X$

$$A_N = \frac{d\sigma^{\uparrow} - d\sigma^{\downarrow}}{d\sigma^{\uparrow} + d\sigma^{\downarrow}}$$

Where $\sigma^{\uparrow}$ and $\sigma^{\downarrow}$ are cross-sections for scattering of a transversely polarised hadron A off an unpolarised proton/lepton/photon, with A polarised upwards and downwards with respect to the production plane.

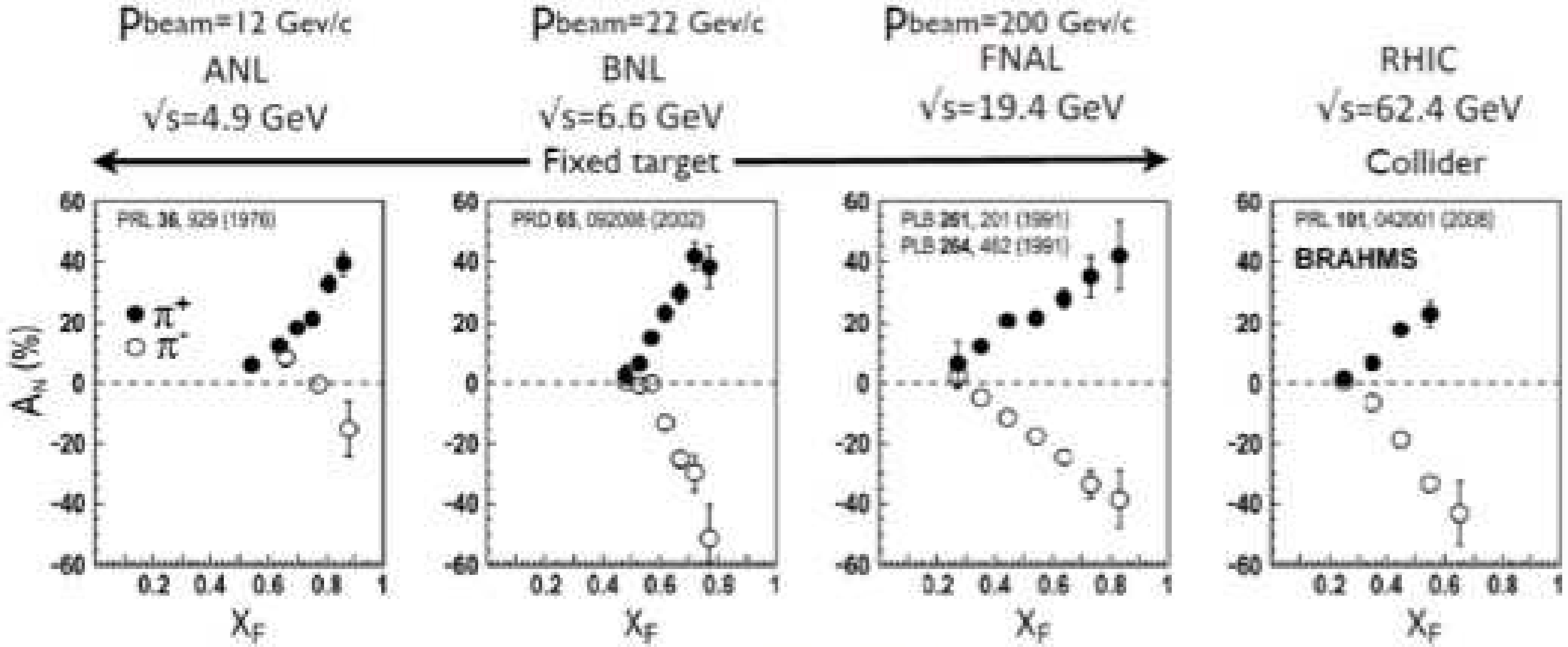

$$x_F = 2p_L/\sqrt{s}$$

Slide from Leonard Gamburg talk, TRANSVERSITY 2011.

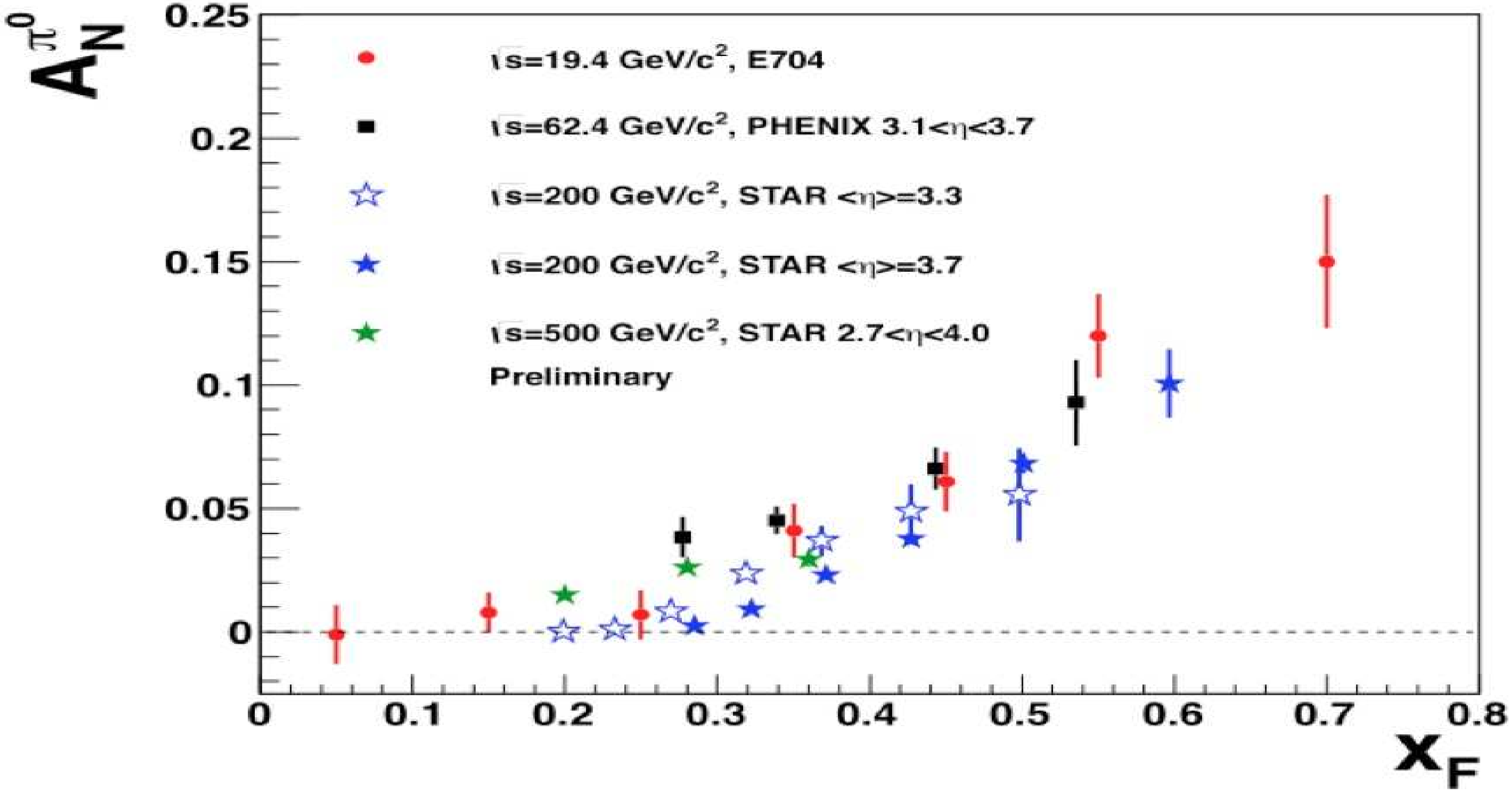

Nice summary plot from the talk of Mriganka and also M. Anslemino, gives extension to highest RHIC energies.

Sivers effect. My own introduction to it: A. Bacchetta, C. Bomhof, U. D'Alesio, P. J. Mulders and F. Murgia, "The Sivers single-spin asymmetry in photon-jet production," Phys. Rev. Lett. **99** (2007) 212002

Two major approaches :

1) Higher twist effects, interaction with spectator quarks, initial and final state interactions. (gauge links)

2)TMD Parton Distribution Function : GPD approach. Out of the many TMD's, Sivers function is the one proposed by D. Sivers to explain the TSSA in hadroproduction of pions. D. Sivers Phys. Rev. D 41 (1990) 83, Phys. Rev. D 43 (1991) 261

This is one of the many TMD's mentioned in the very nice talk by M. Anselmino.

Sivers function encodes the correlation between the azimuthal distribution of an unpolarised parton in a transversely polarised hadron.

TSSA a probe of patron's transverse momentum and spin orbit correlation ?

Understanding the TSSA in the framework of the GPM: Generalised Parton model.

One can not explain the TSSA's in terms of hard scattering without using transverse momentum of the partons in the nucleon, in a parton model approach

Refs. M.Anselmino et al Phys. Rev. D 73, 014020 (2006), U. D'Alesio, F. Murgia,Phys. Rev. D 70, 074009 (2004), M. Anslemino, M. Boglione, U. D'Alesio, E. Leader, F. Murgia Phys. Rev. D 71,014002(2005), U. D'Alesio, F. Murgia, C. Pisano and P. Taels, Phys. Rev. D **96** (2017) no.3, 036011

So what is the parton model that is generalised to get the GPM?

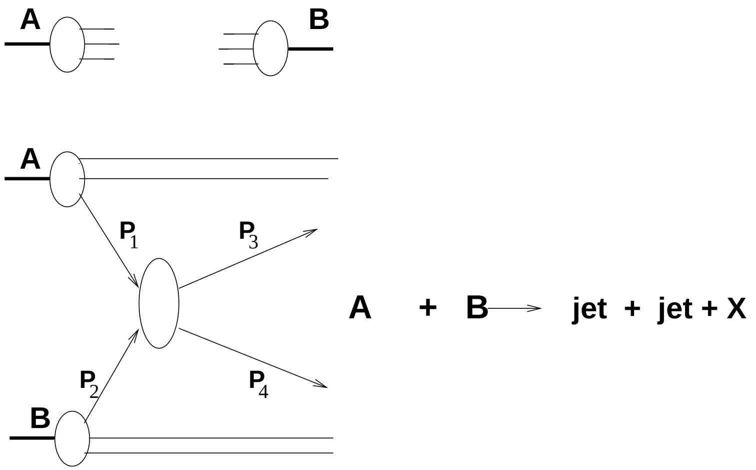

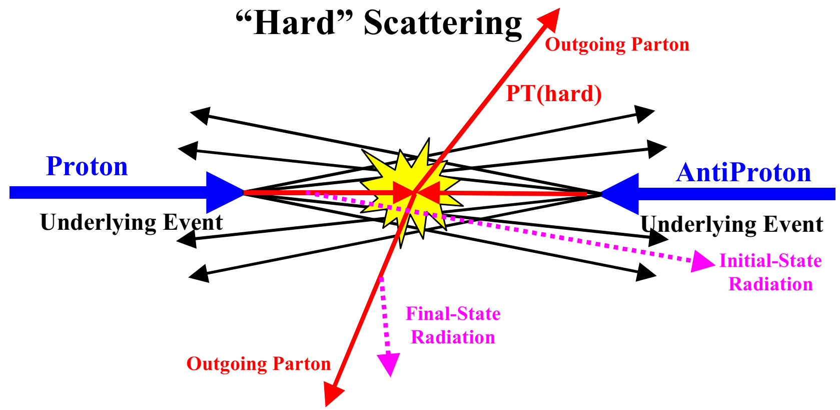

QCD factorisation theorem for short distance, inlcusive processes

$$\sigma(pp \to X + ..) = \sum_{a,b} \int_0^1 dx_1 dx_2 f_a(x_1, \mu_F^2) f_b(x_2, \mu_F^2)$$
$$\times \sigma(a + b \to X) \left(x_1, x_2, \mu_R^2, \alpha_s(\mu_R^2), \alpha(\mu_R^2), \frac{Q^2}{\mu_R^2}, \frac{Q^2}{\mu_F^2} \right)$$

Theoretical prediction:

Initial State	subprocess	final state	
parton density distributions PDF	$\sigma(a + b \to X)$	Fragmentation Functions	Required for large p_T particle production.

For example the expression for the single particle (say C) production at large p_T is given by:

$$\frac{E_C\, d\sigma^{AB\to C,X}}{d^3\vec{p}_C} = \sum_{a,b,c,d} \int dx_{a,b}\, dz\, f_{a/A}(x_a,\mu_f^2) f_{b/B}(x_b,\mu_F^2)\, \frac{d\hat{\sigma}^{ab\to cd}}{d\hat{t}} \frac{\hat{s}}{\pi z^2}\, \delta(\hat{s}+\hat{t}+\hat{u})\, D_{C/c}(z)$$

Both the parton densities and fragmentation functions are k_T integrated and obtained in collinear factorisation.

But SSA's can not be explained in this picture using only collinear factisation picture. G.Kane, W. Repko and J. Pumplin Phys.Rev.Lett. 41 (1978) 1689. Need to include the k_T dependent parton densities and fragmentation functions.

GPM then to my thinking is a phenomenological approach to TMD . In fact the road from Parton Model to QCD improved Parton Model also went through such approaches. There we were helped by 'universailty' OR Process independence of the collinear parton densities. Things are different for TMD's. They may be process dependent.

Strategy: try to see whether one can 'infer' the Sivers functions using data and then test what is measured against various theoretical predictions wherever possible, the increasing our understanding of the 'three dimensional picture' of the Nucleon. (Explained clearly by M. Anselmino yesterday)

TMD approach: pQCD factorization including spin and intrinsic transverse momentum dependent (TMD) effects. TMD factorization established for 1)SIDIS, 2)DY, 3)production of color singlet states and 4)color singlet production in double parton scattering.

In GPM then, for example, inclusive single particle production will be given by:

$$\frac{E_C\, d\sigma^{AB\to C,X}}{d^3\vec{p}_C} = \sum_{a,b,c,d} \int dx_{a,b} d^2\vec{k}_{\perp a,b}\, dz \quad d^3\vec{k}_C\, \delta(\vec{k}_C \cdot \hat{\vec{p}}_c) \hat{f}_{a/A}(x_a, \vec{k}_{\perp a})$$
$$\hat{f}_{b/B}(x_b, \vec{k}_{\perp b}) \frac{\hat{s}}{x_a x_b s} \frac{d\hat{\sigma}^{ab\to cd}}{d\hat{t}}(x_a, x_b, \hat{s}, \hat{t}) \frac{\hat{s}}{\pi} \delta(\hat{s}+\hat{t}+\hat{u}) \frac{1}{z^2}\, J(z, |\vec{k_C}|)\, \hat{D}_{C/c}(z, \vec{k}_C)$$

$\hat{f}$ and $\hat{D}$ are the transverse momentum dependent PDF s and fragmentation functions respectively.

$$f_{i/p}(x, k_\perp; Q) = f_{i/p}(x, Q) \frac{1}{\pi \langle k_\perp^2 \rangle} e^{-k_\perp^2/\langle k_\perp^2 \rangle}$$

The numerator in computation of TSSA is written as convolution of the Quark Sivers Function(QSF) with subprocesses involving quarks and convolution of the Gluon Sivers Function with subprocesses involving gluons.

Sivers function:

$$\hat{f}_{q/p^\uparrow}(x, \boldsymbol{k}_\perp) = f_{q/p}(x, k_\perp) + \frac{1}{2}\Delta^N f_{q/p^\uparrow}(x, k_\perp)\boldsymbol{S}\cdot(\hat{\boldsymbol{P}}\times\hat{\boldsymbol{k}}_\perp),$$

$$\Delta^N f_{i/p^\uparrow}(x, k_\perp; Q) = 2\mathcal{N}_i(x) f_{i/p}(x, Q) h(k_\perp)\frac{e^{-k_\perp^2/\langle k_\perp^2\rangle}}{\pi\langle k_\perp^2\rangle}$$

with,

$$\mathcal{N}_i(x) = N_i x^{\alpha_i}(1-x)^{\beta_i}\frac{(\alpha_i+\beta_i)^{\alpha_i+\beta_i}}{\alpha_i^{\alpha_i}\beta_i^{\beta_i}}$$

and

$$h(k_\perp) = \sqrt{2e}\frac{k_\perp}{M_1}e^{-k_\perp^2/M_1^2}$$

QSF's determined by fits to the data on SSA in SIDIS and DY, using just DGLAP evolution M. Anselmino et al, Phys. Rev. D79,054010,(2009) and Phys. Rev. D 72, 094007..... and using TMD evolution 1107.4446, Phys. Rev. D 86, 014028 (2012)....

The idea has been extract the QSF from SIDIS and apply first to see how well one an explain the TSSA in hadroporduction of π.

Even though no formal proof exists the data seemed to be understandable in terms of QSF extracted from SIDIS.

- describes experimental data on unpolarised cross-sections for $pp \to \gamma, \pi + X$ (upto a K-factor) better than collinear LO or NLO calculations.
  U. D'Alesio and F. Murgia, Phys. Rev. D70 074009 (2004) [hep-ph/0408092] and references 2-4 therein
  J. Huston *et al.*, Phys. Rev. D51 6139
  J.F. Owens, Rev. Mod. Phys. 59, 465 (1987)
- provides a good description on SSA in $p^{\uparrow}p \to \pi + X$ (in the forward region) over a wide range of c.m energies. M. Boglione, U. D'Alesio and F. Murgia, Phys. Rev. D77 051502 [0712.4240]
  U. D'Alesio and F. Murgia, Phys. Rev. D70 074009 (2004) [hep-ph/0408092]
  U. D'Alesio and F. Murgia, Prog.Part.Nucl.Phys. 61 394-454 (2008) [0712.4328]

Gluons are the all important probe for studying QCD. SO what do we know about the Gluon Sivers Function?

In the absence of any information early works we used two models for GSF, following Boer and Vogelsang.

I.e. use the same $k_\perp$ dependency as QSF and use

$$A : \mathcal{N}_g(x) = (\mathcal{N}_u(x) + \mathcal{N}_d(x))/2, \quad B : \mathcal{N}_g(x) = \mathcal{N}_d(x)$$

When I will show you plots it will be called BV(A), BV(B).

A first indirect estimate of the GSF, in a GPM framework was performed by D'Alesio, Murgia and Pisano:

U. D'Alesio, F. Murgia, and C. Pisano, JHEP 09, 119 (2015) [1506.03078]

- They fit the GSF to midrapidity data on pion production, $p^{\uparrow}p \to \pi^0 + X$ at RHIC.
- The QSFs used in the extraction were fit to earlier SIDIS data.

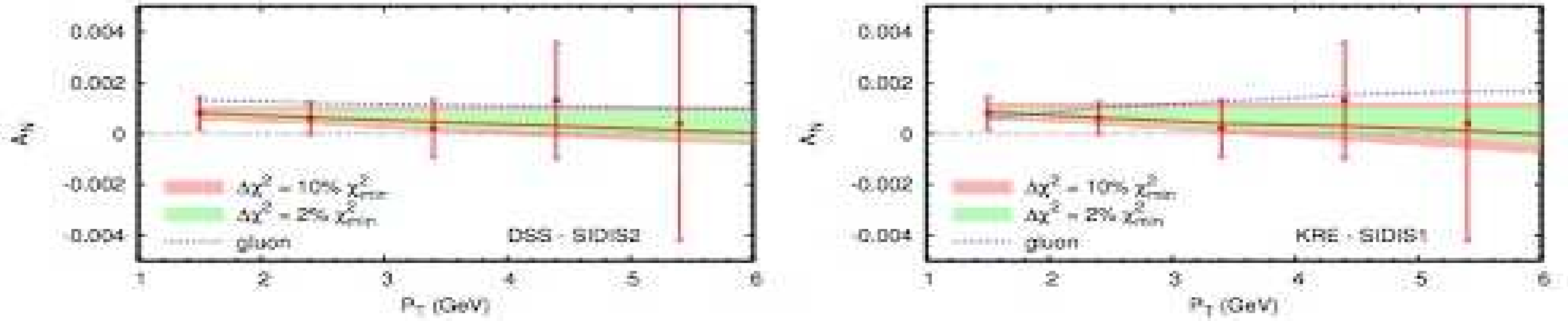

Both fits describe PHENIX pion production data very well!

One fit uses kaon-pion segregated data and hence sea densities are needed to be included in the fits and other one uses all charged particles.

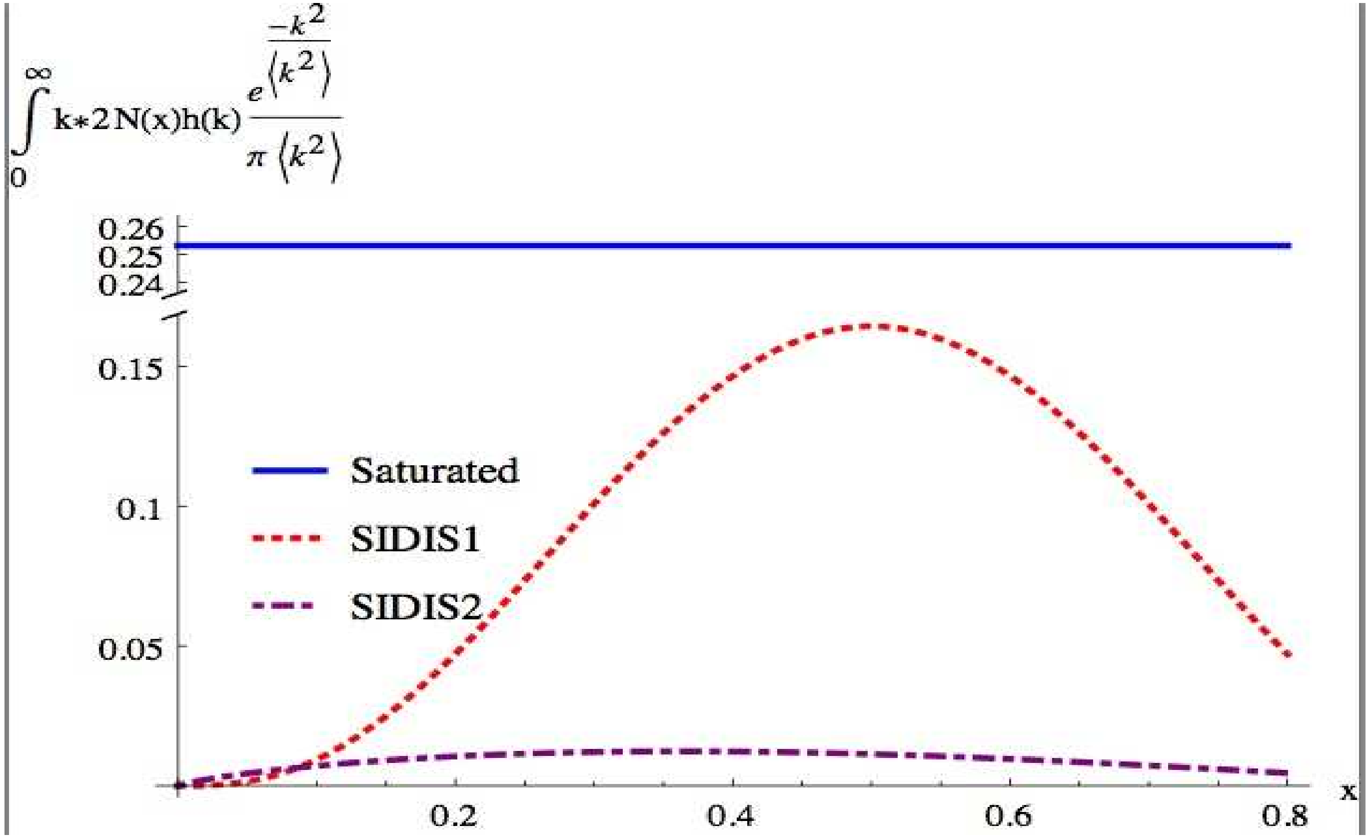

Can one have 'direct' probes of gluon Sivers Function?

Choose final states where the gluon will contribute dominantly.

History : Final states which dominated gluon determination contain heavy quarks, Either charmonium or open charm production in DIS or in pp or pA collsions.

For γp or $\gamma^* p$ initial states (photo production and DIS) the subprocess is

$$\gamma + g_p \rightarrow Q + \bar{Q}, \gamma^* + g_p \rightarrow Q + \bar{Q}$$

At LO, once you choose your kinematic region well, heavy quark production receives contribution ONLY from gluons in the proton.

In pp collisions, mainly due to color factors

$gg \rightarrow Q + \bar{Q}$ dominates over the $q\bar{q} \rightarrow Q + \bar{Q}$, certainly for charm which is the heavy flavour we consider.

I] Inclusive production of J/ψ and D in $ep^{\uparrow}$

$e + p^{\uparrow} \to e + J/\psi + X$ and $e + p^{\uparrow} \to e + D + X$ where the the γ is quasi-real.

II] Inclusive production of J/ψ and D in $pp^{\uparrow}$

$p + p^{\uparrow} \to e + J/\psi + X$ and $p + p^{\uparrow} \to e + D + X$ where the the γ is quasi-real.

Open heavy charm production, i.e D meson production in $pp^{\uparrow}$ was proposed by M. Anselmino et al Phys. Rev. D70, 074025 (2004) [hep-ph/0407100].

Their study considered two options : The maximum GSF allowed by positivity limit and zero. Showed that at RHIC this can be sensitive to GSF.

More recently work done on Color Gauge Invariant version of GPM. Phys. Rev. D96, 036011 (2017).

J/ψ production better over open charm because open charm does receive some contribution from quarks. One needs to be alive to this. Also need to choose kinematic region that contribution from intrinsic charm is small!

However, correct model for charmonium production is not yet fixed by the unpolarised data from fixed target and collider experiments still. D meson production on the other hand needs fragmentation of the c quark which is available from fits to earlier data.

The statistics higher for open charm compared to closed charm J/ψ measurement very clean.

The probes are complementary.

$$d\sigma^{\uparrow} - d\sigma^{\downarrow} = \int dx_{\gamma} dx_g d^2\vec{k}_{\perp\gamma} d^2\vec{k}_{\perp g} \Delta^N f_{g/p}(x_g, \vec{k}_{\perp g}) f_{\gamma/e}(x_{\gamma}, \vec{k}_{\perp\gamma})$$

We use a trick which was used by M. Anselmino et al in their DY paper and one can rewrite the same quantity as an integral over q_T, y of the J/Ψ. The q_T distribution carries an imprint of $k_{\perp g}$ dependency of the Sivers function directly.

We calculate $A_N^{sin(\phi_{q_T} - \phi_S)}$ which involves ntegrals of $d\sigma^{\uparrow} - d\sigma^{\downarrow}$ and $d\sigma^{\uparrow} + d\sigma^{\downarrow}$.

$$d\sigma^{\uparrow} - d\sigma^{\downarrow} = \int d\phi_{q_T} \int q_T dq_T \int_{4m_c^2}^{4m_D^2} [dM^2] \int [d^2\boldsymbol{k}_{\perp g}] \times \Delta^N f_{g/p^{\uparrow}}(x_g, \boldsymbol{k}_{\perp g}) f_{\gamma/e}(x_\gamma, \boldsymbol{q}_T - \boldsymbol{k}_{\perp g}) \times \hat{\sigma}_0(M^2) \sin(\phi_{q_T} - \phi_S) \quad (23)$$

and

$$d\sigma^{\uparrow} + d\sigma^{\downarrow} = 2 \int d\phi_{q_T} \int q_T dq_T \int_{4m_c^2}^{4m_D^2} [dM^2] \int [d^2\boldsymbol{k}_{\perp g}] \times f_{g/p}(x_g, \boldsymbol{k}_{\perp g}) f_{\gamma/e}(x_\gamma, \boldsymbol{q}_T - \boldsymbol{k}_{\perp g}) \times \hat{\sigma}_0(M^2). \quad (24)$$

So it depends on 1) GSF 2)WW function $f_{\gamma/e}(x_\gamma, \vec{k}_{\perp\gamma})$ and 3)the gluon density in unpolarised proton. First study: Use BV models. $k_{\perp g}$ dependence as used in extraction of QSF from SIDIS. Use $\mathcal{N}_u, \mathcal{N}_d$ from the early DGLAP fits. Calculated for JLAB,Hermes, COMPASS and eRHIC energy.

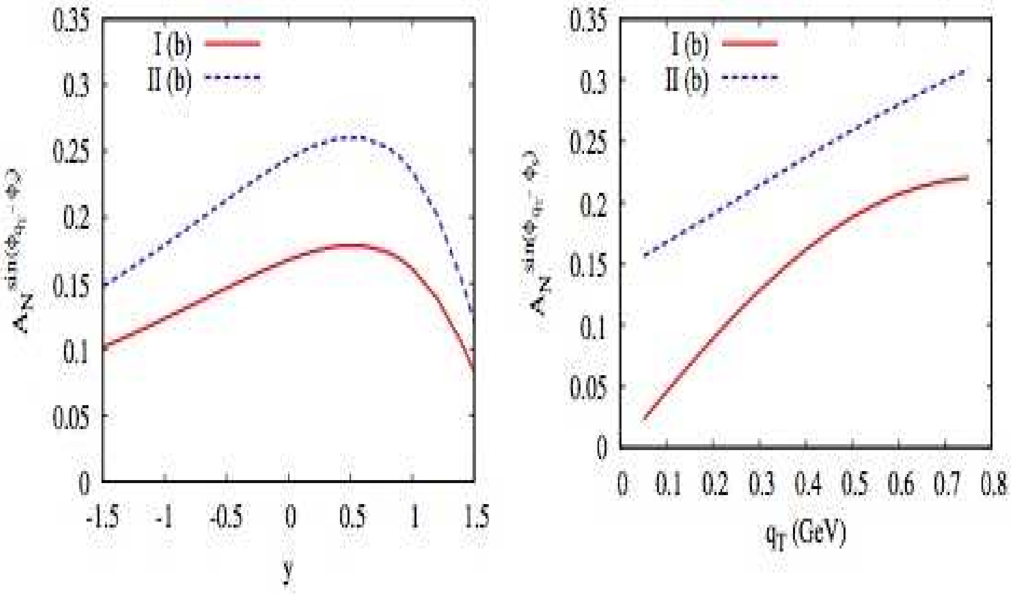

FIG. 7 (color online). The single spin asymmetry $A_N^{\sin(\phi_{q_T}-\phi_S)}$ for the $e + p^{\uparrow} \to e + J/\psi + X$ at COMPASS as a function of y (left panel) and q_T (right panel). The plots are for two models I (solid red line) and II (dashed blue line) with parameterization (b). The integration ranges are $(0 \leq q_T \leq 1)$ GeV and $(0 \leq y \leq 1)$. The results are given at $\sqrt{s} = 17.33$ GeV.

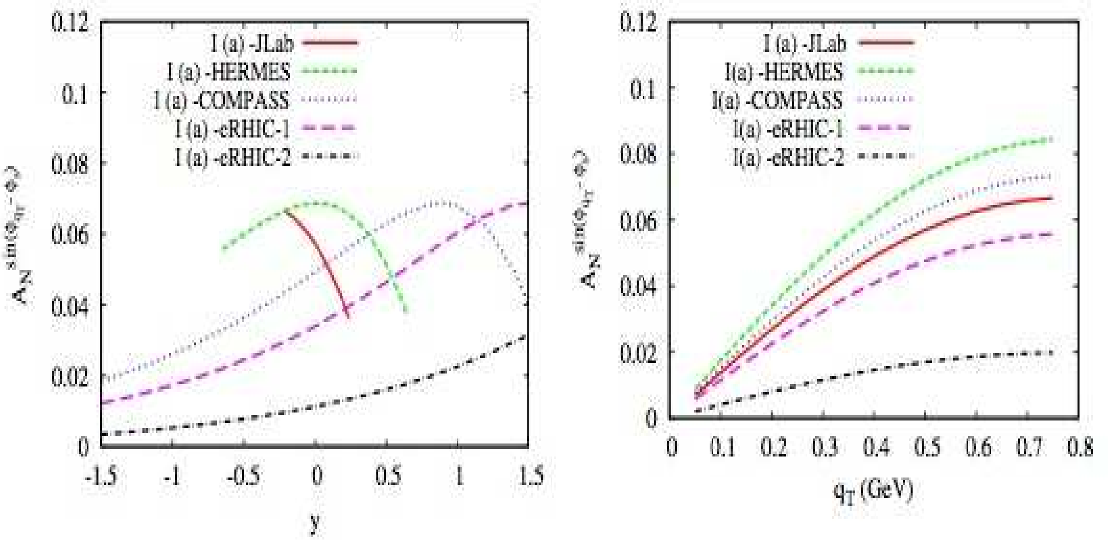

FIG. 8 (color online). The single spin asymmetry $A_N^{\sin(\phi_{q_T}-\phi_S)}$ for the $e + p^{\uparrow} \to e + J/\psi + X$ as a function of y (left panel) and q_T (right panel). The plots are for model I with parameterization (a) compared for JLab ($\sqrt{s}$ = 4.7 GeV) [solid red line], HERMES ($\sqrt{s}$ = 7.2 GeV) [dashed green line], COMPASS ($\sqrt{s}$ = 17.33 GeV) [dotted blue line], eRHIC-1 ($\sqrt{s}$ = 31.6 GeV) [long dashed pink line] and eRHIC-2 ($\sqrt{s}$ = 158.1 GeV) [dot-dashed black line].

GODBOLE *et al.* PHYSICAL REVIEW D **91,** 014005 (2015)

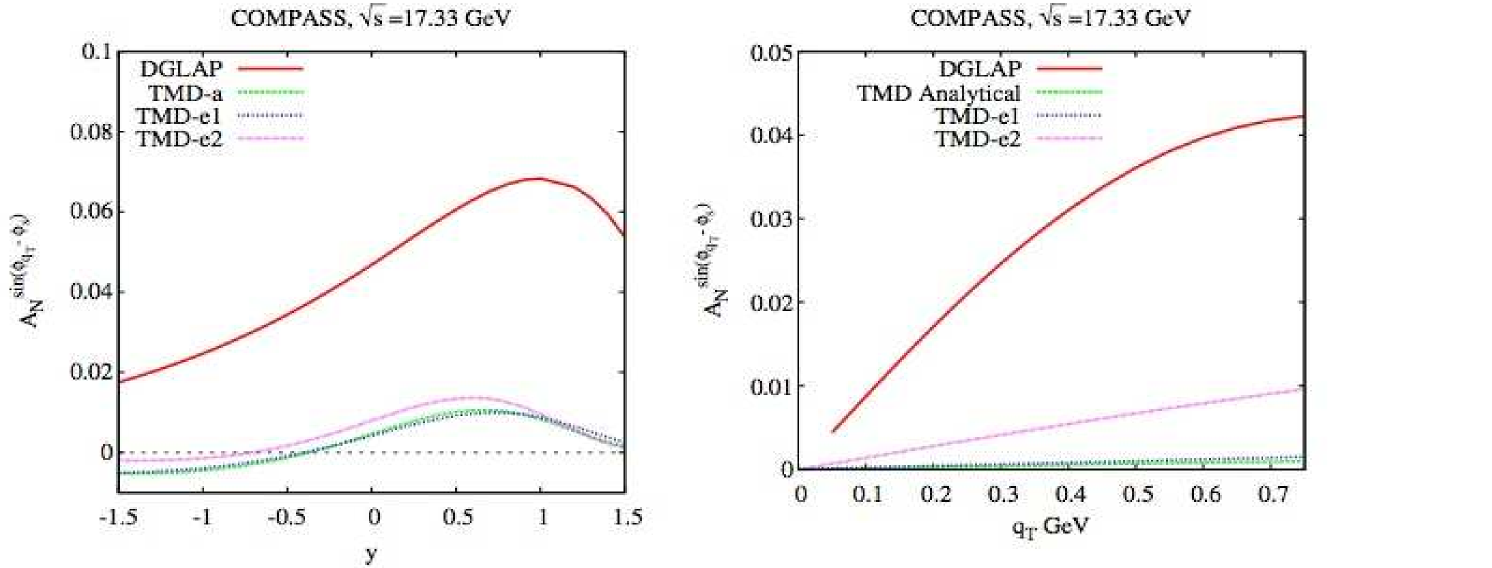

FIG. 4 (color online). COMPASS energy ($\sqrt{s} = 17.33$ GeV), asymmetry as a function of y (left panel) and q_T (right panel) for parametrization (a). The integration ranges are $(0 \leq q_T \leq 1)$ GeV and $(-1.5 \leq y \leq 1.5)$. The convention for the color and line styles is the same as in Fig. 2.

The predictions stable under our varying ways of doing TMD evolution. One was using the analytical result obtained by M. Anselmino et al, in another, due to Echevarria et al, where in the evolution perturbative part is summed upto NLL accuracy. Still with BV A and BV B models. Calculations with DMP fits presented in a Poster.

$$
\begin{aligned}
d\sigma^{\uparrow} - d\sigma^{\downarrow} &= \frac{E_D d\sigma^{p^{\uparrow} p \to DX}}{d^3 \boldsymbol{p}_D} - \frac{E_D d\sigma^{p^{\downarrow} p \to DX}}{d^3 \boldsymbol{p}_D} \\
&= \int dx_a dx_b dz d^2\mathbf{k}_{\perp a} d^2\mathbf{k}_{\perp b} d^3\mathbf{k}_D \delta(\mathbf{k}_D \cdot \hat{\boldsymbol{p}}_c)\delta(\hat{s} + \hat{t} + \hat{u} - 2m_c^2)\mathcal{C}(x_a, x_b, z, \mathbf{k}_D) \\
&\times \Bigg\{ \sum_q \Bigg[\Delta^N f_{q/p^{\uparrow}}(x_a, \mathbf{k}_{\perp a}) f_{\bar{q}/p}(x_b, \mathbf{k}_{\perp b}) \frac{d\hat{\sigma}^{q\bar{q} \to c\bar{c}}}{d\hat{t}}(x_a, x_b, \mathbf{k}_{\perp a}, \mathbf{k}_{\perp b}, \mathbf{k}_D) D_{D/c}(z, \mathbf{k}_D) \Bigg] \\
&+ \Bigg[\Delta^N f_{g/p^{\uparrow}}(x_a, \mathbf{k}_{\perp a}) f_{g/p}(x_b, \mathbf{k}_{\perp b}) \frac{d\hat{\sigma}^{gg \to c\bar{c}}}{d\hat{t}}(x_a, x_b, \mathbf{k}_{\perp a}, \mathbf{k}_{\perp b}, \mathbf{k}_D) D_{D/c}(z, \mathbf{k}_D) \Bigg] \Bigg\},
\end{aligned}
$$

$$
\begin{aligned}
d\sigma^{\uparrow} + d\sigma^{\downarrow} &= \frac{E_D d\sigma^{p^{\uparrow} p \to DX}}{d^3 \boldsymbol{p}_D} + \frac{E_D d\sigma^{p^{\downarrow} p \to DX}}{d^3 \boldsymbol{p}_D} = 2\frac{E_D d\sigma^{pp \to DX}}{d^3 \boldsymbol{p}_D} \\
&= 2\int dx_a dx_b dz d^2\mathbf{k}_{\perp a} d^2\mathbf{k}_{\perp b} d^3\mathbf{k}_D \delta(\mathbf{k}_D \cdot \hat{\boldsymbol{p}}_c)\delta(\hat{s} + \hat{t} + \hat{u} - 2m_c^2)\mathcal{C}(x_a, x_b, z, \mathbf{k}_D) \\
&\times \Bigg\{ \sum_q \Bigg[\hat{f}_{q/p}(x_a, \mathbf{k}_{\perp a}) \hat{f}_{\bar{q}/p}(x_b, \mathbf{k}_{\perp b}) \frac{d\hat{\sigma}^{q\bar{q} \to c\bar{c}}}{d\hat{t}}(x_a, x_b, \mathbf{k}_{\perp a}, \mathbf{k}_{\perp b}, \mathbf{k}_D) \hat{D}_{D/c}(z, \mathbf{k}_D) \Bigg] \\
&+ \Bigg[\hat{f}_{g/p}(x_a, \mathbf{k}_{\perp a}) \hat{f}_{g/p}(x_b, \mathbf{k}_{\perp b}) \frac{d\hat{\sigma}^{gg \to c\bar{c}}}{d\hat{t}}(x_a, x_b, \mathbf{k}_{\perp a}, \mathbf{k}_{\perp b}, \mathbf{k}_D) \hat{D}_{D/c}(z, \mathbf{k}_D) \Bigg] \Bigg\}.
\end{aligned}
$$

Modified the formulation of Mellis et al for solving the kinematics to include finite mass of the fragmenting quark, obtaining a semi analytical method to solve for z. Do the calculation for RHIC 200 GeV, AFTER@LHC -115 GeV and also RHIC - 500 GeV

Quark contribution negligible. Asymmetries small but significant. Rates such that can be measured with a Luminosity of 1 fb^{-1}, applying price in the rate into a μ. See later.

TRANSVERSE SINGLE SPIN ASYMMETRY IN ... PHYSICAL REVIEW D 94, 114022 (2016)

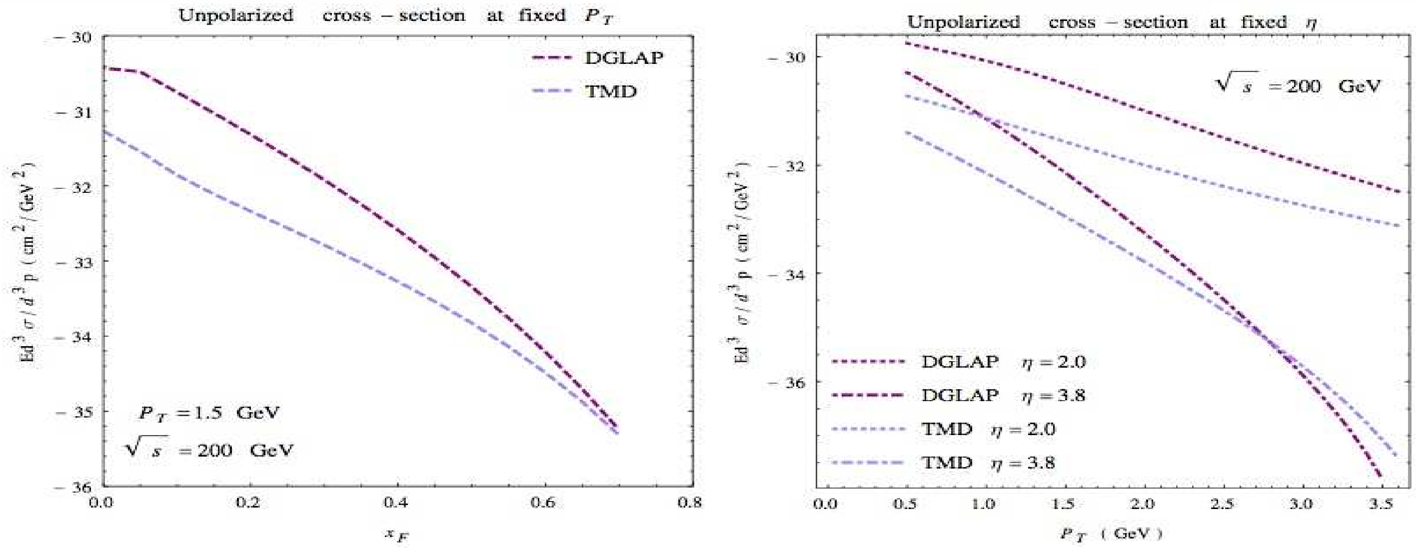

(a) (b)

FIG. 1. Unpolarized cross section: Panel (a) shows the numbers at fixed $P_T = 1.5$ GeV and panel (b) shows the numbers at fixed pseudorapidity values $\eta = 2.0$, 3.8. The red dashed line is for the results obtained using DGLAP evolution with $\langle k_\perp^2 \rangle = 0.25$ GeV^2 (cf. Sec. III) and the blue dotted line denotes the results obtained using TMD evolution (cf. Sec. IV).

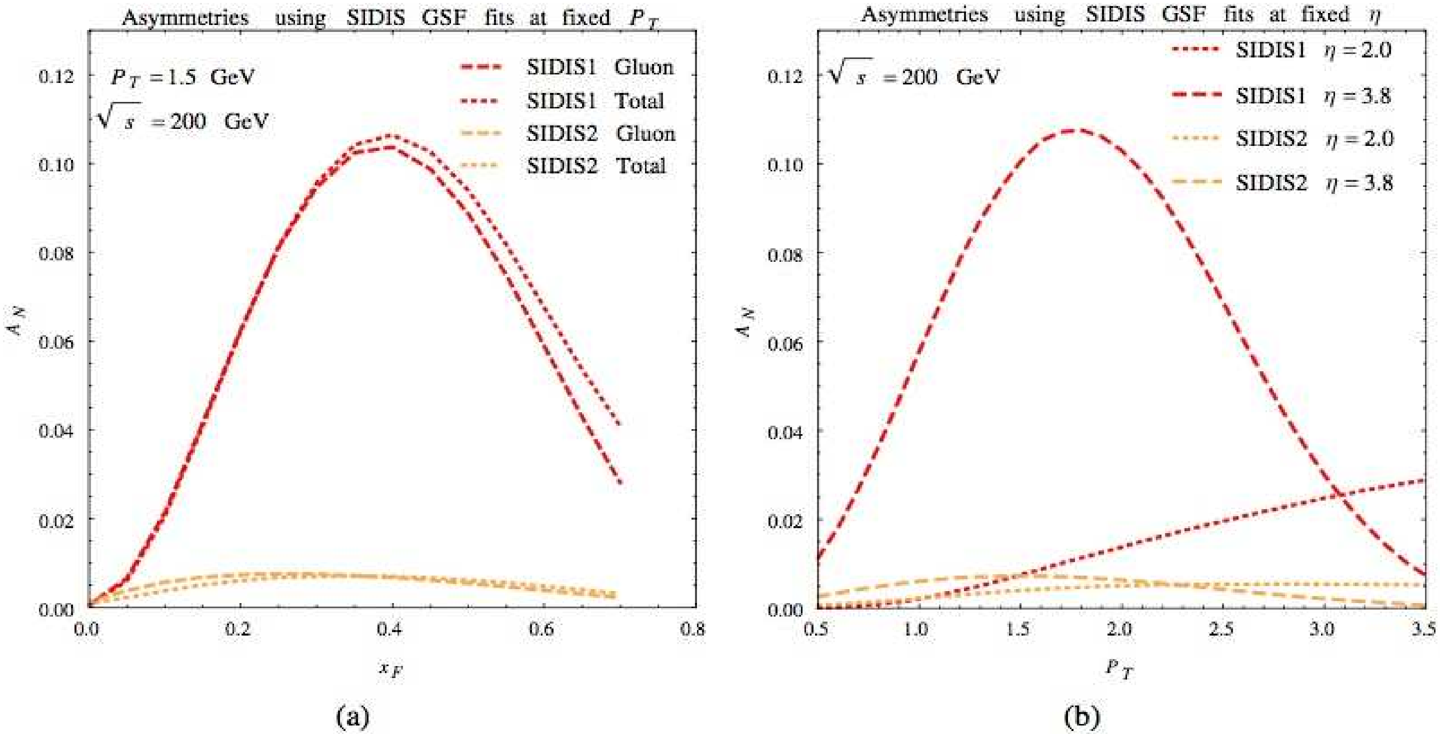

FIG. 2. Asymmetry predictions using the DMP fits: Panel (a) shows results at fixed $P_T = 1.5$ GeV and panel (b) shows results at fixed $\eta = 2.0$, 3.8. Predictions using the SIDIS1 GSF are in red and those using the SIDIS2 GSF are in orange. In the left panel, we show results obtained when the quark contribution is also included. As can be seen, it is relatively small.

GODBOLE, KAUSHIK, and MISRA PHYSICAL REVIEW D 94, 114022 (2016)

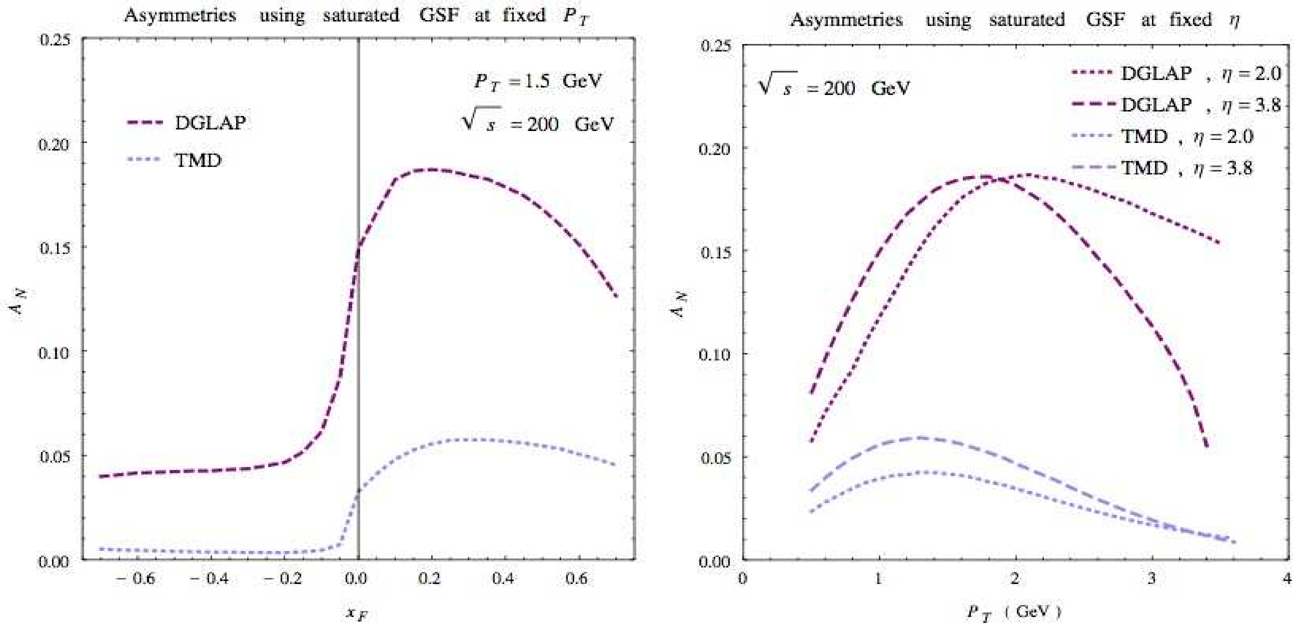

(a) (b)

FIG. 3. Asymmetry predictions using a saturated GSF evolved with DGLAP and TMD evolution: Panel (a) shows results at fixed $P_T = 1.5$ GeV and panel (b) shows results at fixed $\eta = 2.0, 3.8$. Results obtained with DGLAP densities are in violet and those obtained with TMD evolved densities are in blue.

GODBOLE, KAUSHIK, and MISRA PHYSICAL REVIEW D **94,** 114022 (2016)

TABLE II. Integrated asymmetries (0.5 GeV $\leq P_T \leq$ 2.0 GeV, 1.0 $\leq \eta \leq$ 3.8) with the SIDIS1 and SIDIS2 Sivers functions at different c.m. energies. Gluon and quark contributions are listed separately. These asymmetry values are much smaller than those shown in the differential plots since the integration region includes low values of η where the asymmetries are smaller.

$\sqrt{s}$ GeV	σ_{total} mb	$A_{N\text{gluon}}^{\text{SIDIS1}}$	$A_{N\text{quark}}^{\text{SIDIS1}}$	$A_{N\text{gluon}}^{\text{SIDIS2}}$	$A_{N\text{quark}}^{\text{SIDIS2}}$	ΔA_N (statistical)
115	3.1×10^{-3}	5×10^{-2}	-6.7×10^{-4}	8.6×10^{-3}	-1.4×10^{-3}	3×10^{-3}
200	8.6×10^{-3}	3.5×10^{-2}	-5.5×10^{-4}	7.3×10^{-3}	-8.5×10^{-4}	1.8×10^{-3}
500	3×10^{-2}	1.4×10^{-2}	-2.5×10^{-4}	5.4×10^{-3}	-3.3×10^{-4}	1×10^{-3}

Formulation very similar to low virtuality lepto production except we have to now fold with partons in the proton rather than with the photon in electron. Results for y dependence

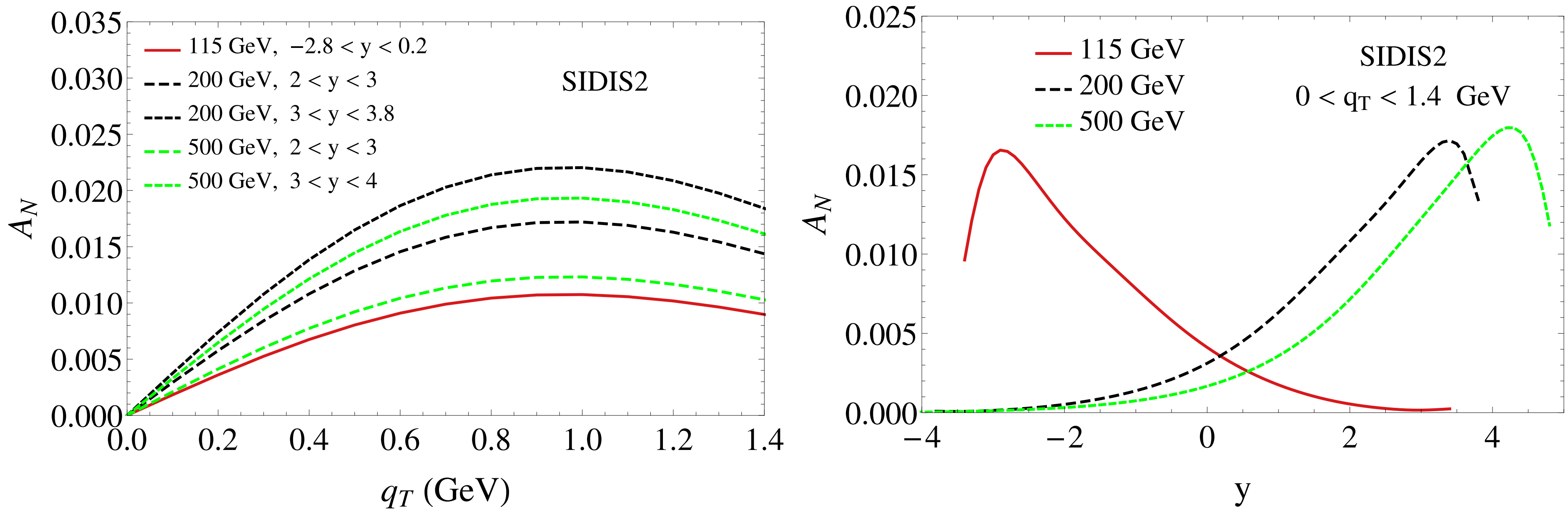

Comparison with Phenix results: Data with large errors unable to draw any conclusions. No statement can be made about GSF and/or TMD/DGLAP (not shown here)

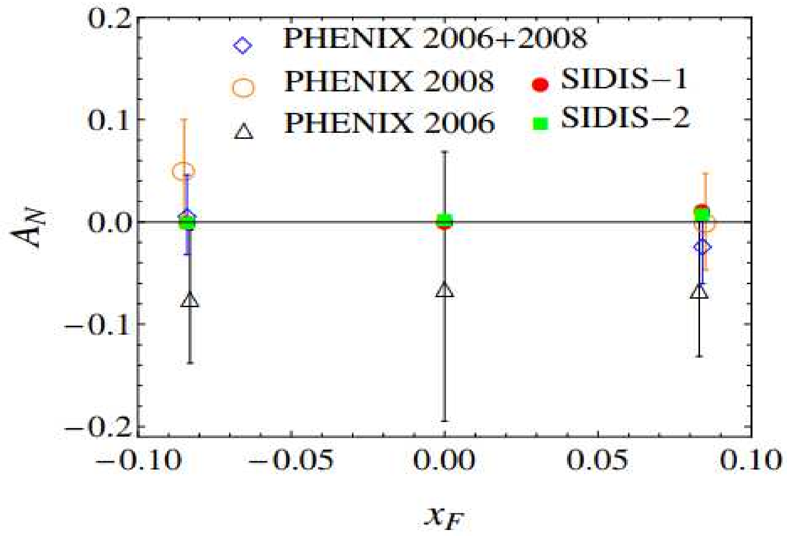

FIG. 7: Comparison of PHENIX measurements [36] of TSSA in $p+p^{\uparrow} \to J/\psi + X$ with predictions obtained using the DMP fits, SIDIS1 and SIDIS2 [33]. The points for the combined (2006 +2008) data have been offset by 0.01 in x_F for visibility. Asymmetry measurements are in the forward ($1.2 < y < 2.2$), backward ($-2.2 < y < -1.2$) and midrapidity ($|y| < 0.35$) regions with $0 \le q_T \le 1.4$ GeV.

Region	$\langle x_F \rangle$	$x^{\uparrow}$ region	$\sigma_{J/\psi} \times$ B.R($\mu^+\mu^-$) (nb)	δA_N	A_N^{SIDIS1}	A_N^{SIDIS2}
$-2.2 < y < 3.8$	0.036	0.002 - 0.7	144.0	0.0026	0.014	0.0055
$1.2 < y < 2.2$	0.086	0.05 - 0.14	29.6	0.0058	0.012	0.0092
$2 < y < 3$	0.186	0.12 - 0.32	18.2	0.0074	0.069	0.013
$3 < y < 3.8$	0.39	0.32 - 0.7	2.45	0.020	0.22	0.017

TABLE IV: Results for cross-section and asymmetry at RHIC1 energy ($\sqrt{s} = 200$ GeV), along with expected statistical error (assuming 1 pb^{-1} of data) and approximate x-region probed. All numbers given with cuts on lepton rapidity: $-2.2 < y_l < 4.0$. Transverse momentum region: $0 \leq q_T \leq 1.4$ GeV.

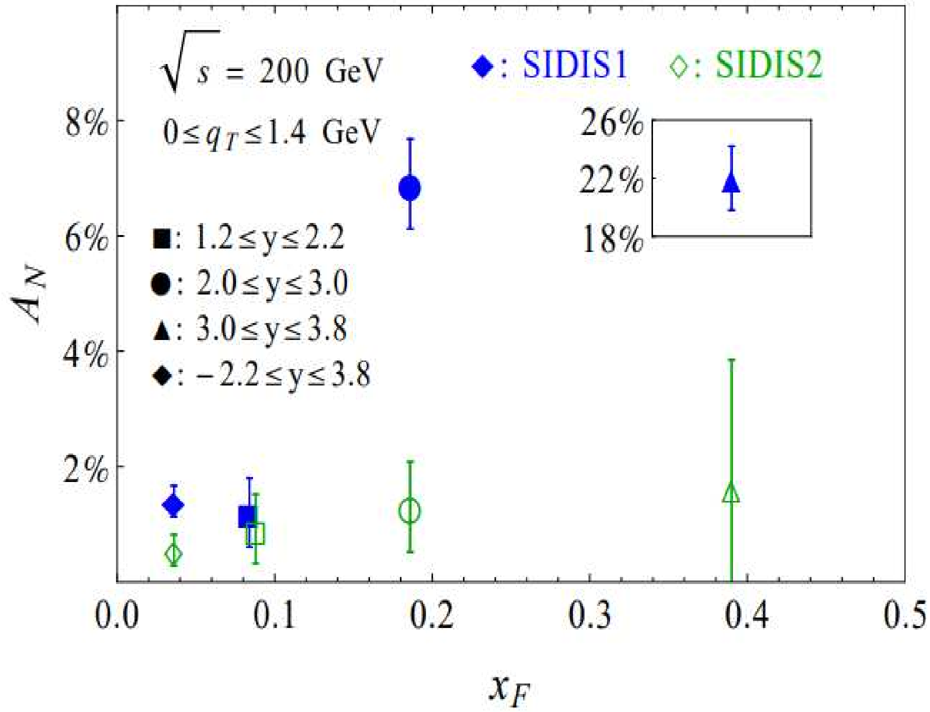

FIG. 9: Predictions for asymmetry in forward region that would be accessible with the fsPHENIX upgrade [47, 48]. Error bars indicate expected statistical errors calculated assuming 1 pb^{-1} of data.

To be done:

1)A better treatment of the k_T dependence of the WW for $ep^{\uparrow}$.

2)Study the effect of CGI GPM